Journal of
Manufacturing and Materials Processing

MDPI

Article

Leveraging Intelligent Machines for Sustainable and Intelligent Manufacturing Systems

Somkiat Tangjitsitcharoen [1], Nattawut Suksomcheewin [1] and Alessio Faccia [2,*]

[1] Department of Industrial Engineering, Faculty of Engineering, Chulalongkorn University, Phayathai Road, Patumwan, Bangkok 10330, Thailand; somkiat.ta@eng.chula.ac.th (S.T.); nattawut.sscw@gmail.com (N.S.)
[2] School of Business, University of Birmingham Dubai, Dubai PO Box 341799, United Arab Emirates
* Correspondence: a.faccia@bham.ac.uk

Abstract: This study presents an intelligent machine developed for real-time quality monitoring during CNC turning, aimed at improving cutting efficiency and reducing production energy. A dynamometer integrated into the CNC machine captures decomposed cutting forces using the Daubechies wavelet transform. These force ratios are correlated with key workpiece dimensions: surface roughness, average roughness, straightness, and roundness. Two predictive models—nonlinear regression and a feed-forward neural network with Levenberg–Marquardt backpropagation—are employed to estimate these parameters under varying cutting conditions. Experimental results indicate that nonlinear regression models outperform neural networks in predictive accuracy. The proposed system offers effective in-process control of machining quality, contributing to shorter cycle times, lower defect rates, and more sustainable manufacturing practices.

Keywords: intelligent machine; digital lean; sustainable and intelligent manufacturing; smart factory; turning; neural network; nonlinear regression

check for updates

Academic Editor: Hyung Wook Park

Received: 17 March 2025
Revised: 25 March 2025
Accepted: 2 April 2025
Published: 6 May 2025

Citation: Tangjitsitcharoen, S.; Suksomcheewin, N.; Faccia, A. Leveraging Intelligent Machines for Sustainable and Intelligent Manufacturing Systems. *J. Manuf. Mater. Process.* **2025**, *9*, 153. https://doi.org/10.3390/jmmp9050153

Copyright: © 2025 by the authors. Licensee MDPI, Basel, Switzerland. This article is an open access article distributed under the terms and conditions of the Creative Commons Attribution (CC BY) license (https://creativecommons.org/licenses/by/4.0/).

1. Introduction

Presently, digital lean manufacturing (DLM) and the intelligent machine tool (IMT) have become more important at the core of the intelligent manufacturing system (IMS) to promote and drive sustainable and intelligent manufacturing (SIM) in the near future, in which in-process monitoring and quality control are normally applied to achieve the SIM system, as shown in Figure 1. Since intelligent machines can help eliminate waste and carbon dioxide, especially from rework processes, this reflects the digital lean and leads to the smart factory [1,2]. Consequently, the smart supply chain can be optimised and planned with smart logistics for smart energy, which can be finally developed into the smart city to reduce the CO_2 emissions for calculating the carbon footprint of products. Hence, this paper presents the advanced works [3,4] of the author to continue and propose an intelligent CNC turning method to monitor the average surface roughness, the surface roughness, the straightness, and the roundness of the workpieces concurrently, which are the critical dimensions of precision parts.

However, those dimensions, which depend on the combinations of cutting conditions, cannot be measured and estimated directly during in-process turning. Therefore, it is necessary to examine the cutting conditions to predict all dimensions, which are the desired parameters of the final workpiece, in order to reduce rejection, rework and production energy for sustainable and intelligent manufacturing systems [5,6].

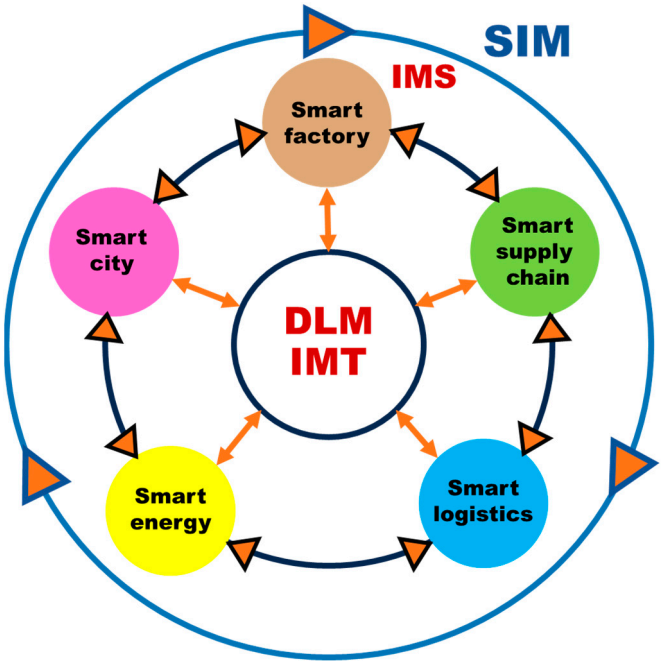


Figure 1. Illustration of digital lean manufacturing and intelligent machine tool driving sustainable and intelligent manufacturing.

The in-process prediction of surface roughness, straightness, and roundness in the CNC turning process has been proposed by an artificial neural network using a decomposed cutting force ratio [4–6]. However, the proposed system has never been compared with the nonlinear regression models [7,8]. Moreover, the nonlinear models have not been utilised to generate the in-process prediction models of those parameters at the same time as the combination of cutting conditions [9–11]. Many researchers have investigated the critical dimensions [12,13], the cutting parameters [14,15], the cutting forces [16], and the workpiece quality [17]. The Daubechies wavelet transform has been adopted recently to decompose the dynamic cutting forces to monitor the signals which correspond with the surface roughness, straightness, and roundness, respectively, in time and frequency domains [18,19].

Therefore, this paper presents the continued work of the author to compare the in-process monitoring and prediction of surface roughness, straightness, and roundness simultaneously between nonlinear regression models and an approach using an artificial neural network, as shown in Figure 2.

Referring to the literature reviews [20–23], the decomposed cutting forces (Fx, Fy, Fz) can filter out the desired signals to specific levels of the wavelet transform, such as the signals of surface roughness, straightness, and roundness [24,25]. As a consequence, the roughness of the surface, the straightness, and the roundness can be estimated based on those decomposed cutting forces [26–29]. However, they have not been monitored and calculated simultaneously in the CNC turning process in the past [30,31].

In order to realise an intelligent CNC turning machine for a sustainable and intelligent manufacturing system, the in-process monitoring system is proposed to forecast the average surface roughness, the surface roughness, the straightness, and the roundness concurrently [32–36]. The nonlinear regression models are employed to represent the relations of the tool wear, the average surface roughness, the surface roughness, the roundness, the cutting conditions, and the ratios of decomposed cutting forces by utilising regression analysis [37–39]. Finally, the experimentally obtained models will be compared to the artificial neural network to compute all critical dimensions during in-process CNC turning,

as shown in Figure 2. The new in-process monitoring system is illustrated to predict the average surface roughness, the surface roughness, the straightness, and the roundness simultaneously by utilising the decomposed cutting forces, as shown in Figure 3.

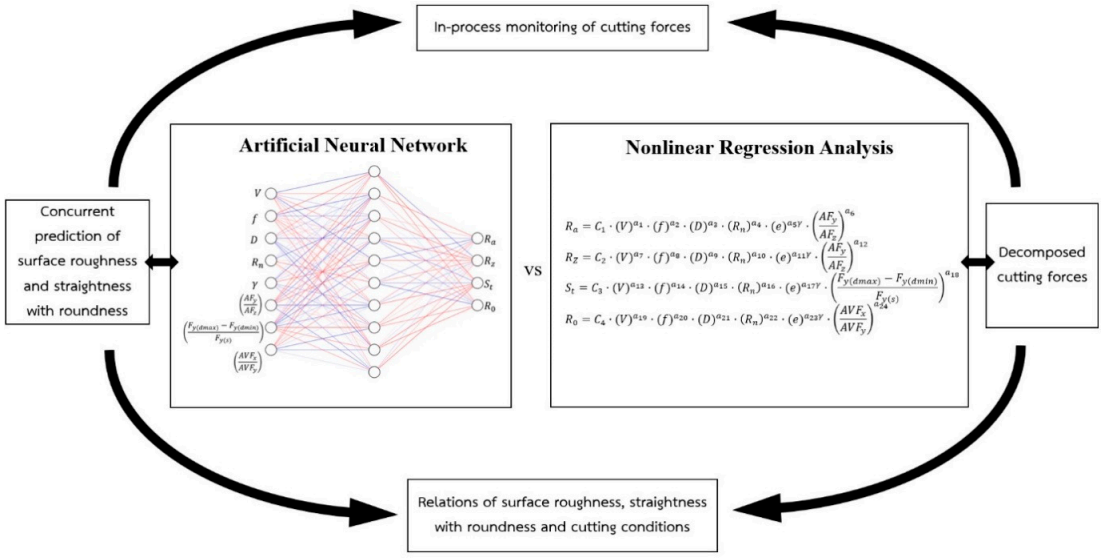


Figure 2. Comparison of in-process monitoring and prediction of surface roughness, straightness, and roundness simultaneously between artificial neural network and nonlinear regression models.

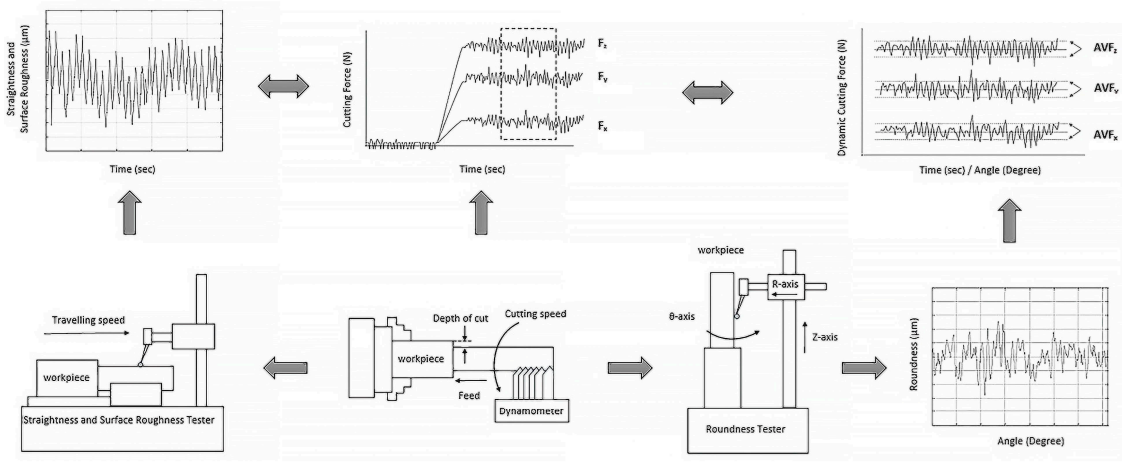


Figure 3. Illustration of a new in-process monitoring system to predict the average surface roughness, the surface roughness, the straightness, and the roundness simultaneously.

Unlike previous studies [40,41], this study uniquely compares nonlinear regression and neural networks for in-process prediction of all critical geometrical parameters (Ra, Rz, St, Ro) simultaneously, based on cutting force decomposition under varying cutting conditions. Prior works addressed one or two parameters independently and did not integrate predictive performance across all four.

2. Relations of Decomposed Cutting Forces Versus Surface Roughness with Straightness and Roundness

According to the theoretical surface roughness, the decomposed feed force is most sensitive to the surface roughness and straightness profiles, which are the same as the feed rate direction [42,43]. The feed rate and the tool nose radius generally create the feed marks on the machined surface [44–47]. The profile of surface roughness can be represented by

the straightness profile, which is the same. Their profiles can be obtained at the same frequency during measuring. However, the roundness profile corresponds with the decomposed radial force (Fx) [48], and the roundness error is normal for the decomposed feed force (Fy) [49].

Preliminary experiments are conducted to monitor the relations of decomposed feed force, decomposed radial force, surface roughness, straightness, and roundness profiles simultaneously [50,51], which are measured off-line using the roundness tester, the straightness and surface roughness tester, as shown in Figure 3. An example of an experimentally obtained profile of surface roughness and straightness versus the decomposed feed force on the 8th level separated from the chip breaking and noise signals is illustrated in Figure 4 with the use of a cutting speed of 200 m/min, feed rate of 0.15 mm/rev, depth of cut of 0.4 mm, tool nose radius of 0.4 mm and rake angle of 11°. The profile of surface roughness and straightness occurs at the frequency of 33 Hz, which is consistent with the amplitude of decomposed feed force, which happens at the same frequency in the frequency domain, as shown in Figure 4. Consequently, the experimentally decomposed radial force and the corresponding roundness profile are illustrated in Figure 5.

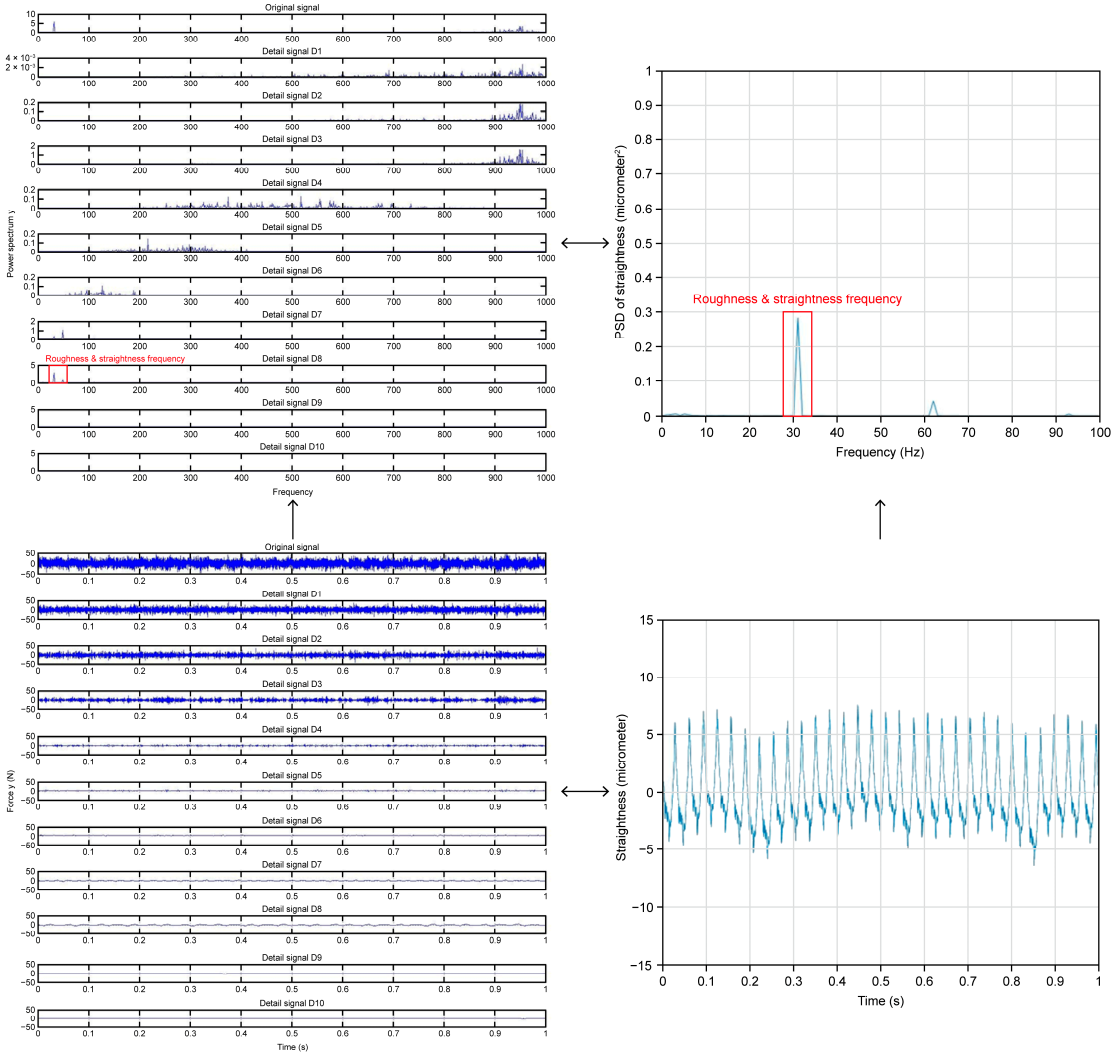


Figure 4. Example of the experimentally obtained profile of surface roughness and straightness versus decomposed feed force in the time domain and their power spectrum density (PSD) in the frequency domain from a cutting speed of 200 m/min, feed rate of 0.15 mm/rev, depth of cut of 0.4 mm, tool nose radius of 0.4 mm and rake angle of 11°.

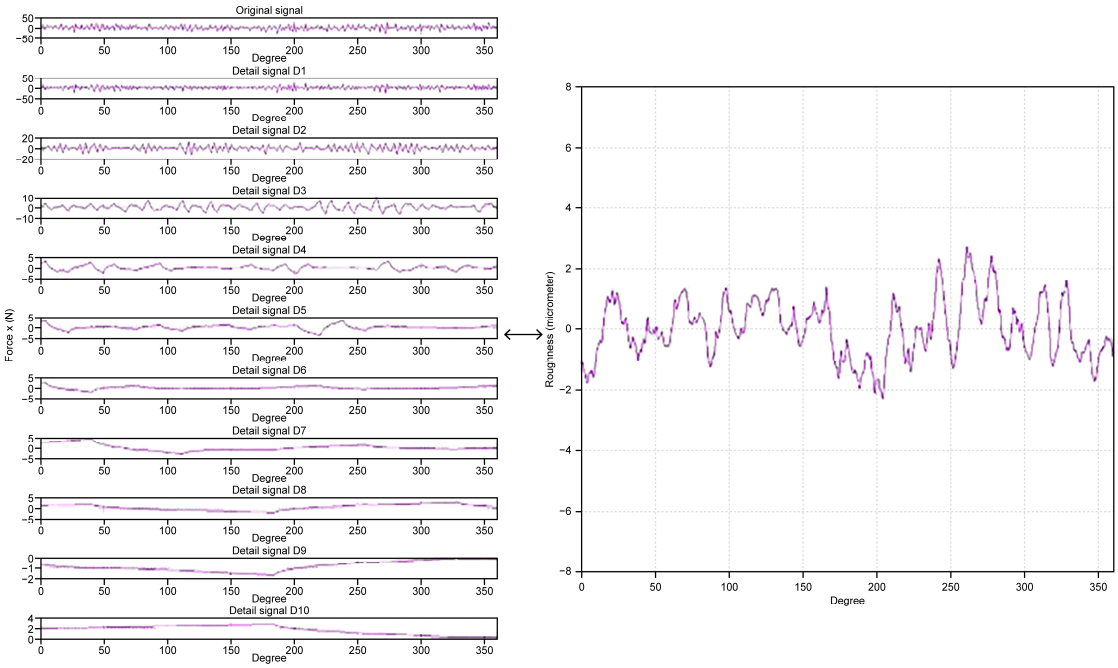


Figure 5. Example of experimentally decomposed radial force and roundness profile from cutting speed of 200 m/min, feed rate of 0.15 mm/rev, depth of cut of 0.4 mm, tool nose radius of 0.4 mm and rake angle of 11°.

The Daubechies wavelet transform can decompose the cutting forces and identify the frequency of specific parameters such as surface roughness, straightness, and roundness, respectively [52,53]. However, the cutting conditions may affect the decomposed cutting forces in predicting those parameters. It is, therefore, necessary to eliminate those combinations of cutting conditions from the decomposed cutting forces. Hence, the distance of maximum peak $F_{y(dmax)}$ to minimum valley $F_{y(dmin)}$ of the decomposed feed force is considered to calculate the straightness error, as shown in Figure 6. However, the distance of the maximum peak to the minimum valley is dimensionless by taking its ratio to its static feed force $(F_{y(dmax)} - F_{y(dmin)})/F_{y(s)}$. The ratio of the area of that decomposed feed force AF_y to that of decomposed main force AF_z is generalised and adopted to estimate the surface roughness. The trapezoidal rule is applied to compute the areas of that ratio (AF_y/AF_z). The roundness error can be forecasted by normalising and taking the ratio of the average variance of decomposed radial force to that of decomposed feed force (AVF_x/AVF_y) [49].

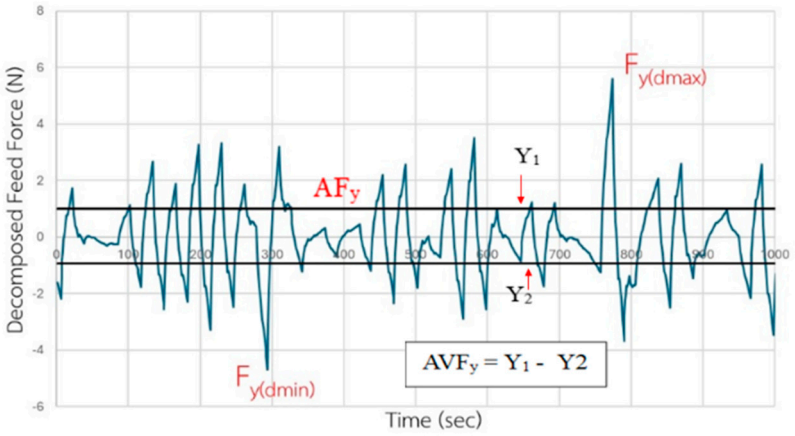


Figure 6. Example of experimentally decomposed feed force from cutting speed of 100 m/min, feed rate of 0.15 mm/rev, depth of cut of 0.4 mm, tool nose radius of 0.4 mm and rake angle of −6°.

3. In-Process Prediction of Surface Roughness and Straightness with Roundness

To estimate the surface roughness, straightness and roundness during the CNC turning process concurrently, the in-process prediction models of those parameters have been newly proposed and developed in terms of exponential forms which have been employed to generate those models with the ratio of decomposed feed force to decomposed main force (AFy/AFz), ratio of the peak-to-valley amplitude of decomposed feed force to its static feed force (Fy(dmax) − Fy(dmin))/Fy(s), and the ratio of the average variance of decomposed radial force to that of the decomposed feed force (AVFx/AVFy). Statistical testing, both a normality test and independent test with variance stability test, will be introduced to validate the experimentally obtained data and models as reliable at the 95% confidence level.

The effects of combinations of cutting conditions, which are the cutting speed, the depth of cut, the feed rate, the nose radius, and the rake angle, are considered in order to compare the effectiveness and prediction accuracy of the experimentally obtained models with the results of the neural network approach. Hence, the relations of the average surface roughness, the surface roughness, the straightness, the roundness, the cutting conditions, and the ratio of decomposed cutting forces are expressed below:

$$R_a = C_1 \cdot (V)^{a_1} \cdot (f)^{a_2} \cdot (D)^{a_3} \cdot (R_n)^{a_4} \cdot (e)^{a_5\gamma} \cdot \left(\frac{AF_y}{AF_z}\right)^{a_6} \quad (1)$$

$$R_Z = C_2 \cdot (V)^{a_7} \cdot (f)^{a_8} \cdot (D)^{a_9} \cdot (R_n)^{a_{10}} \cdot (e)^{a_{11}\gamma} \cdot \left(\frac{AF_y}{AF_z}\right)^{a_{12}} \quad (2)$$

$$S_t = C_3 \cdot (V)^{a_{13}} \cdot (f)^{a_{14}} \cdot (D)^{a_{15}} \cdot (R_n)^{a_{16}} \cdot (e)^{a_{17}\gamma} \cdot \left(\frac{F_{y(dmax)} - F_{y(dmin)}}{F_{y(s)}}\right)^{a_{18}} \quad (3)$$

$$R_o = C_4 \cdot (V)^{a_{19}} \cdot (f)^{a_{20}} \cdot (D)^{a_{21}} \cdot (R_n)^{a_{22}} \cdot (e)^{a_{23}\gamma} \cdot \left(\frac{AVF_x}{AVF_y}\right)^{a_{24}} \quad (4)$$

where R_a is the average surface roughness in μm, R_z is the surface roughness in μm, S_t is the straightness error in μm, R_o is the roundness error in μm, V is the cutting speed in m/min, f is the feed rate in mm/rev, R_n is the tool nose radius in mm, D is the depth of cut in mm, and γ is the rake angle in degree.

Meanwhile, a1 to a24 and C1 to C4 are the powers and coefficients of the models, respectively, which are obtained based on the experimentally obtained data by applying the nonlinear regression analysis and the least square method at a 95% confidence level. It is supposed that the proposed in-process models can predict all dimensions effectively during the CNC turning process simultaneously, which has never been compared with the neural network approach before.

On the other hand, the Levenberg–Marquardt neural network and feed-forward back-propagation algorithm with eight inputs [54–56] are utilised to train with those required dimensions to investigate the prediction accuracy compared with the above models, as shown in Figure 2. The major cutting conditions, which are the cutting speed, the depth of cut, the feed rate, the tool nose radius, and the rake angle, are important inputs to predict those parameters simultaneously. The in-process monitoring system between the neural network approach and nonlinear regression analysis has never been performed before to calculate those dimensions concurrently. It is understood that the proposed system can predict all critical parameters well during in-process CNC turning to achieve sustainable and intelligent manufacturing in the future.

4. Experimental Setup and Cutting Conditions

The cutting experiments for nonlinear regression analysis are executed on the MAZAK CNC turning (4-axis NEXUS 200MY/MSY). Plain carbon steel (S45C) and coated carbide tools are adopted to prove the proposed method by using the different tool nose radiuses and rake angles. The major cutting conditions of 214 runs are presented in Table 1. The neural network system will be optimised, referring to the minimum prediction error or the maximum correlation coefficient (R), and after that, the ratio of experiments for the neural network approach will be set as training, testing, and validation, respectively. Consequently, the experimentally obtained results are executed and evaluated at the same time.

Table 1. Major cutting conditions.

Parameter	Value
Cutting Tool	Coated Carbide
Workpiece	S45C
Cutting Speed (m/min)	100, 150, 180, 200, 260
Feed Rate (mm/rev)	0.1, 0.15, 0.2, 0.25, 0.3
Depth of Cut (mm)	0.2, 0.4, 0.5, 0.6, 0.8
Nose Radius (mm)	0.4, 0.8
Rake Angle (degree)	–6, +11

Figure 7 shows the MAZAK 4-axis CNC turning centre, where the Y-axis allows off-centre machining and the live tooling on the turret facilitates complex profiles. Specifications include a max spindle speed of 5000 rpm and a tool turret with 12 stations.

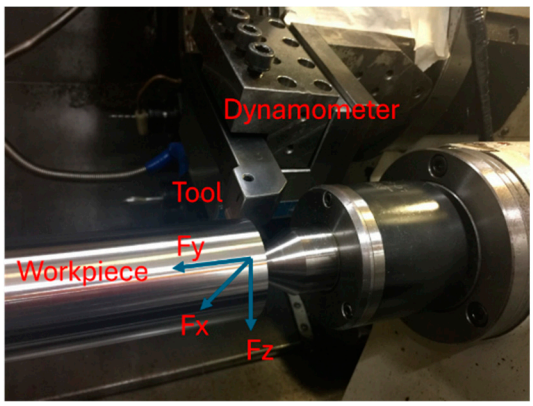


Figure 7. Illustration of the dynamometer and experimental setup.

The dynamometer (Kistler model: 9121 - The Kistler Model 9121, a quartz 3-component toolholder dynamometer, manufactured by Kistler Instrumente AG, headquartered in Winterthur, Switzerland) is attached to the turret of the CNC turning machine with a sampling rate of 10 kHz and a low-pass filtered frequency of 5 kHz before applying the Daubechies wavelet transform to obtain the decomposed cutting forces, as shown in Figure 7. The dynamometer is calibrated, and hence, the decomposed cutting forces are promising in computing the average surface roughness, surface roughness, straightness, and roundness. The straightness and surface roughness tester (Mitutoyo SJ-400) and the roundness tester (TSK, model: Rondcom43c) are adopted to measure the machined surface roughness, straightness, and roundness error, respectively. The cutting tests start with new cutting conditions for each coated carbide tool.

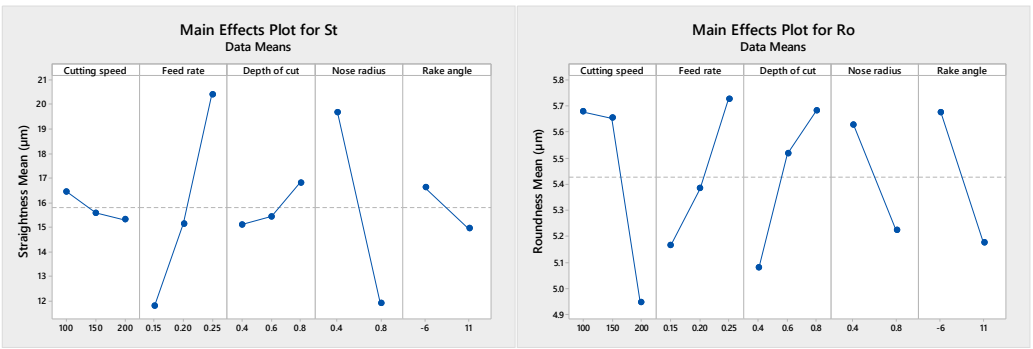
The following procedures are introduced to fit Equations (1)–(4) and train the neural network system to obtain the weights in the hidden layers, which are finally set to 10 for better processing time and accuracy.

(1) Record the decomposed cutting forces under the major cutting conditions.
(2) Monitor the corresponding time records of the surface roughness, straightness, and roundness profile with the decomposed cutting forces in the time and frequency domains.
(3) Measure the surface roughness, straightness, and roundness profiles for each cutting condition.
(4) Compute the ratios of decomposed cutting forces of $\frac{AF_y}{AF_z}$, $\frac{F_{y(dmax)}-F_{y(dmin)}}{F_{y(s)}}$, and $\frac{AVF_x}{AVF_y}$ on the 8th level of the wavelet transform, respectively.
(5) Analyse the experimental data from steps (1) to (4) before optimising models (1) to (4) by utilising statistical analyses.
(6) Determine the feed-forward backpropagation neural network system for the average surface roughness (Ra), the surface roughness (Rz), the straightness (St), and the roundness (Ro) with the ratios of decomposed cutting forces under major cutting conditions to obtain the highest prediction accuracy or correlation coefficient (R).
(7) Verify and compare the experimentally obtained equations from the above step (5) with the neural network system from step (6).

The neural network consisted of a feed-forward architecture with 1 hidden layer of 10 neurons, trained using the Levenberg–Marquardt backpropagation algorithm. Inputs include V, f, D, Rn, rake angle, and decomposed force ratios. The data were split as 80% training, 10% validation, and 10% test.

5. Experimental Results and Discussions

The experimentally obtained results of average surface roughness, surface roughness, straightness and roundness show the same trend when the cutting conditions are changed. Therefore, an example of experimentally obtained straightness and roundness versus the cutting conditions is illustrated in Figure 8. It is understood that as the cutting speed increases, the straightness and roundness errors decrease because the work material becomes softer due to the higher cutting temperature, which leads to lower cutting forces. As a result, the straightness and roundness errors might be less at the higher cutting speed. The above reasons can also help explain an improvement in surface roughness when cutting at a higher speed. Each experimental condition was repeated three times, and average values were taken. The standard deviation was <5% across all measurements, confirming high repeatability.



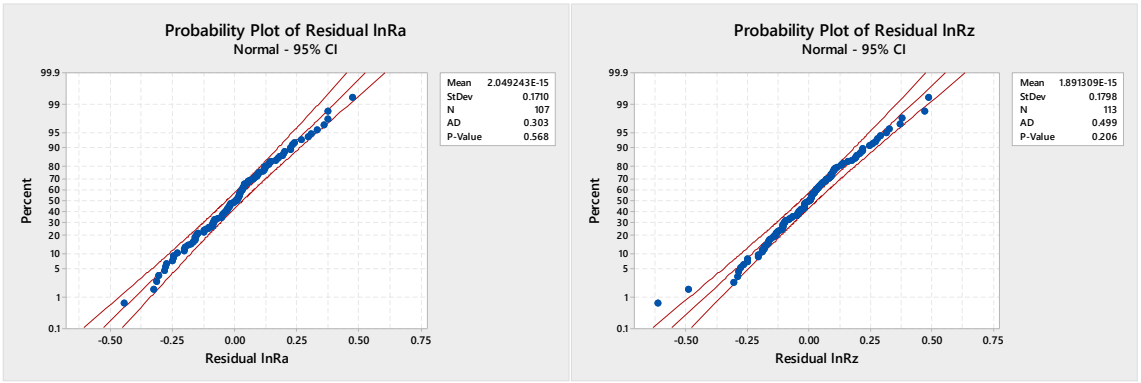
(**a**) (**b**)

Figure 8. Example of experimentally obtained straightness and roundness versus cutting conditions. (**a**) Straightness error (St); (**b**) roundness error (Ro).

An increase in feed rate and depth of cut causes high straightness and roundness errors due to the larger cutting forces, as a result of the increase in straightness and roundness errors. It is concluded that the larger tool nose radius can improve the straightness and roundness errors because the areas of feed marks, which have remained on the surface finish, are eliminated by the contacting area between the tool nose radius and the machined surface, which can also explain the better surface roughness. The higher rake angle results in better chip flowability as a consequence of the lower cutting force. Therefore, the straightness and roundness errors are also reduced.

Firstly, the experimentally obtained data need to be validated by statistical analyses before generating the in-process prediction models and training the neural network system [8,14,48], as shown in Figure 2. These analyses include the normal test, the independent test, and the variance test, respectively.

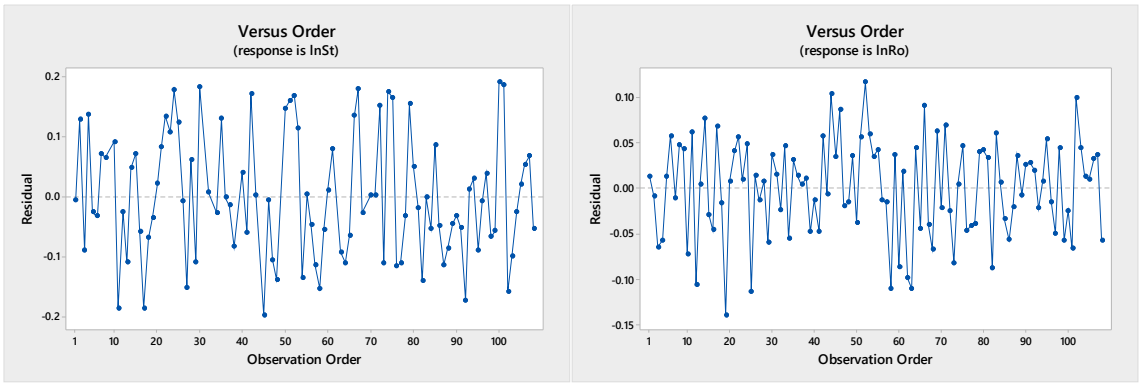
The example of experimentally obtained normal distributions of average surface roughness and surface roughness shows that the experimentally obtained data lie on the linear line, as shown in Figure 9. Their p-values are 0.568 and 0.206, which are more than 0.05 at a significance level of 0.05 (α = 0.05). Therefore, it is understood that the experimentally obtained data of average surface roughness and surface roughness are normally distributed. The experimentally obtained normal distributions of straightness and roundness have the same trends and p-values of 0.056 and 0. 112, which are higher than 0.05, respectively. It can be concluded that the residuals have a normal distribution.



(**a**) (**b**)

Figure 9. Example of experimentally obtained normal distributions of average surface roughness and surface roughness. (**a**) Normal test of average surface roughness (Ra); (**b**) normal test of surface roughness (Rz).

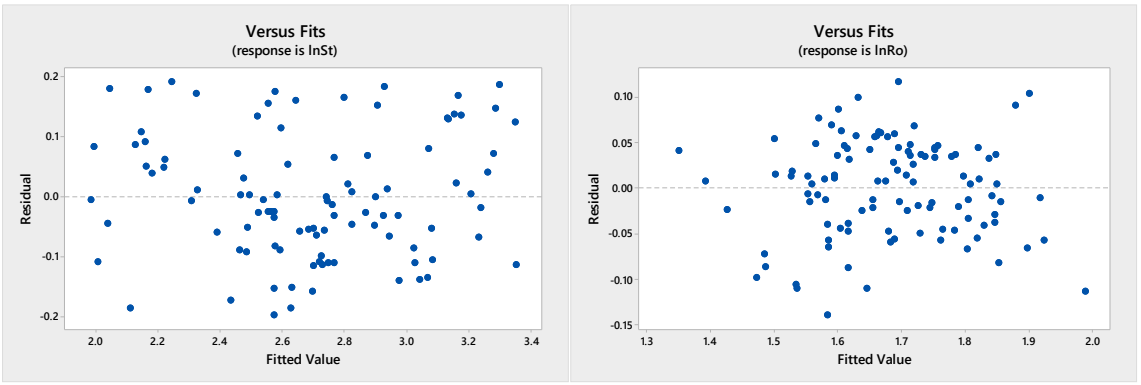
The experimentally obtained independent test is a test to measure the data distribution. The example of experimentally obtained data of straightness and roundness is illustrated by the residual versus the observation order, as shown in Figure 10. The deviations of the experimentally obtained data are independent and not certain patterns. The experimentally obtained data are uniformly distributed on the zero line. In summary, the experimentally obtained independent tests of straightness and roundness have good data independence. Furthermore, the experimentally obtained data of average surface roughness and surface roughness are also independent, respectively.



(**a**) (**b**)

Figure 10. Example of experimentally obtained independent tests of straightness and roundness. (**a**) Independent test of straightness (St); (**b**) independent test of roundness (Ro).

Figure 11 illustrates an example of experimentally obtained variance tests, which present the relation between residual and fitted values of straightness and roundness. The experimentally obtained data appear as a random scatter around the zero-center line; as a result, the experimentally obtained data are independent. Hence, the assumption of equal variance becomes valid because the common variance and mean value are zero. Moreover, the residual is independent not only of straightness and roundness but also of average surface roughness and surface roughness.



(**a**) (**b**)

Figure 11. Example of experimentally obtained variance tests of straightness and roundness. (**a**) Variance test of straightness (St); (**b**) variance test of roundness (Ro).

When referring to the above statistical analyses, it is understood that the experimentally obtained data can be used to develop reliable models, and there are no outliers in the experimentally collected data. The nonlinear forms of Equations (1)–(4) are converted and computed firstly by taking the logarithmic transformation, as shown in Equations (5)–(8). The regression coefficients are obtained based on the actual cutting results by utilising the nonlinear regression analysis with the least square method.

$$lnR_a = 3.718 - 0.19lnV + 1.3961lnf + 0.0796lnD - 0.6401lnR_n - 0.01391\gamma - 0.289ln\left(\frac{AF_y}{AF_z}\right) \quad (5)$$

$$lnR_z = 5.207 - 0.2012lnV + 1.2917lnf + 0.1357lnD - 0.6514lnR_n - 0.00807\gamma - 0.295ln\left(\frac{AF_y}{AF_z}\right) \quad (6)$$

$$lnS_t = 4.531 - 0.0910lnV + 1.1638lnf + 0.0841lnD - 0.7127lnR_n - 0.00679\gamma - 0.079ln\left(\frac{F_{y(dmax)} - F_{y(dmin)}}{F_{y(s)}}\right) \quad (7)$$

$$lnR_o = 2.138 - 0.0819lnV + 0.0888lnf + 0.0571lnD - 0.0609lnR_n - 0.004671\gamma + 0.3048ln\left(\frac{AVF_x}{AVF_y}\right) \quad (8)$$

The above Equations (5)–(8) are substituted by the natural logarithm and transformed to the original exponential form, as shown in Equations (9)–(12). We can be confident that the experimentally obtained models of in-process prediction of average surface roughness, surface roughness, straightness, and roundness are practicable and valid at a high significance (p-value = 0.000) at a 95% confidence level. Therefore, the proposed nonlinear models are believable and useful to predict the in-process average surface roughness, surface roughness, straightness and roundness, respectively, by utilising the cutting conditions and in-process monitoring of decomposed cutting forces as the predictors.

$$R_a = e^{3.718} \cdot V^{-0.19} \cdot f^{1.3961} \cdot D^{0.0796} \cdot {R_n}^{-0.6401} \cdot e^{-0.01391\gamma} \cdot \left(\frac{AF_y}{AF_z}\right)^{-0.289} \quad (9)$$

$$R_Z = e^{5.207} \cdot V^{-0.2012} \cdot f^{1.2917} \cdot D^{0.1357} \cdot {R_n}^{-0.6541} \cdot e^{-0.0807\gamma} \cdot \left(\frac{AF_y}{AF_z}\right)^{-0.295} \quad (10)$$

$$S_t = e^{4.531} \cdot V^{-0.0910} \cdot f^{1.1638} \cdot D^{0.0841} \cdot {R_n}^{-0.7127} \cdot e^{-0.00679\gamma} \cdot \left(\frac{F_{y(dmax)} - F_{y(dmin)}}{F_{y(s)}}\right)^{-0.079} \quad (11)$$

$$R_o = e^{2.138} \cdot V^{-0.0819} \cdot f^{0.0888} \cdot D^{0.0571} \cdot {R_n}^{-0.0609} \cdot e^{-0.00467\gamma} \cdot \left(\frac{AVF_x}{AVF_y}\right)^{0.3048} \quad (12)$$

The signs and amplitudes of the powers in Equations (9)–(12) present the direction and effect of cutting conditions and ratios of $\frac{AF_y}{AF_z}$, $\left(\frac{F_{y(dmax)} - F_{y(dmin)}}{F_{y(s)}}\right)$, and $\frac{AVF_x}{AVF_y}$ on the average surface roughness, the surface roughness, the straightness, and the roundness, respectively. It is noticed that the average surface roughness, surface roughness, and straightness will be improved when the ratios of $\frac{AF_y}{AF_z}$ and $\left(\frac{F_{y(dmax)} - F_{y(dmin)}}{F_{y(s)}}\right)$ increase due to the negative power, as shown in Equations (9)–(11). Vice versa, the roundness becomes worse while the ratio of $\frac{AVF_x}{AVF_y}$ progresses as its power is positive, as shown in Equation (12).

The in-process monitoring and quality control of average surface roughness, surface roughness, straightness, and roundness are simultaneously compared between nonlinear regression models and artificial neural networks in Figure 2. The artificial neural network is required to train and optimise the system. After optimising the neural network system to obtain the closest prediction values or the highest correlation coefficient (R), the ratio of experiments for the neural network approach is decided as training of 80%, validation of 10%, and test of 10%, respectively, as shown in Figure 12. The experimentally obtained correlation coefficients (R) of training, validation, and test of the neural network system are 0.995, 0.95, and 0.989, respectively. It is interpreted that all parameters of average roughness, roughness, straightness, and roundness can be predicted simultaneously with the ratios of $\frac{AF_y}{AF_z}$, $\left(\frac{F_{y(dmax)} - F_{y(dmin)}}{F_{y(s)}}\right)$, and $\frac{AVF_x}{AVF_y}$ during the in-process CNC turning. Hence, the experimentally obtained results from the trained neural network system will be compared and checked at the same time as the experimentally obtained results from in-process prediction models.

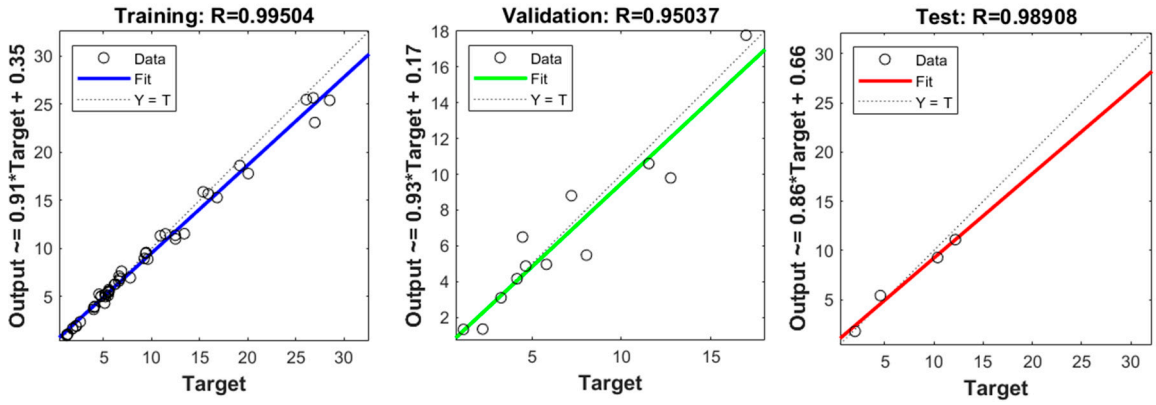


Figure 12. Illustration of training, validation and test of a neural network system to predict the average roughness, surface roughness, straightness, and roundness concurrently.

The confirmation tests are introduced to validate and verify the prediction accuracy of the in-process prediction models and the trained neural network, as shown in Table 2. Figures 13–16 illustrate the experimentally measured average roughness, surface roughness, straightness, and roundness versus the experimentally predicted ones from the trained neural network and nonlinear regression models, respectively. It is understood that the average roughness, surface roughness, straightness, and roundness can be well estimated by in-process prediction models, which are closer to the measured ones than the ones from trained neural networks. A comparison of prediction accuracy between trained neural networks and nonlinear regression models is summarised in Table 3. It is implied that the nonlinear regression models can forecast the average roughness, the surface roughness, the straightness, and the roundness simultaneously during in-process CNC turning, which has a higher prediction accuracy of over 90% than the ones from the trained neural network by utilising the ratios of $\frac{AF_y}{AF_z}$, $\left(\frac{F_{y(dmax)}-F_{y(dmin)}}{F_{y(s)}}\right)$, and $\frac{AVF_x}{AVF_y}$.

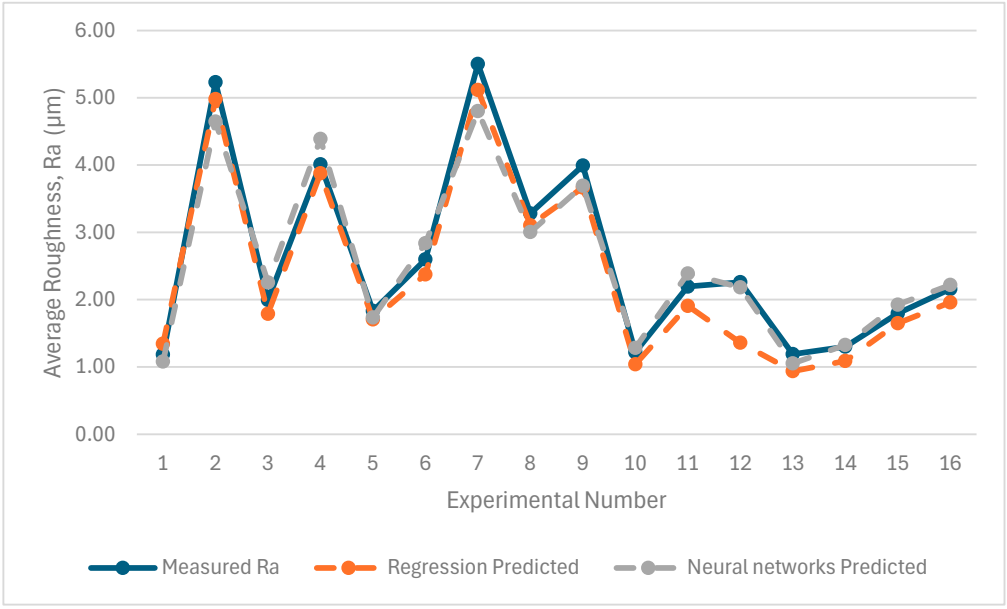


Figure 13. Illustration of measured average surface roughness versus predicted average roughness obtained from nonlinear regression model and trained neural network.



Figure 14. Illustration of measured surface roughness versus predicted surface roughness obtained from nonlinear regression model and trained neural network.

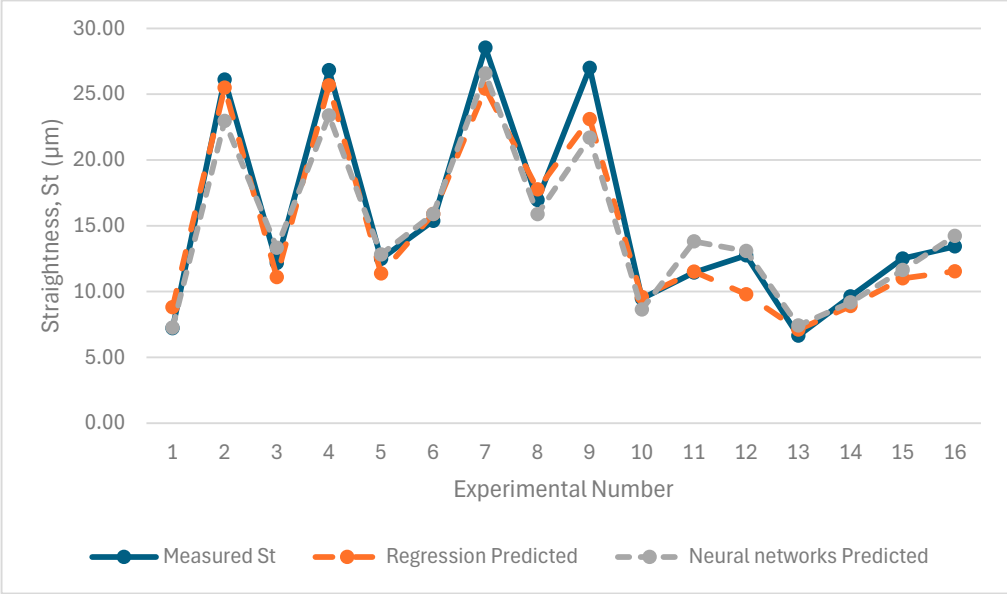


Figure 15. Illustration of measured straightness versus predicted straightness obtained from nonlinear regression model and trained neural network.

Table 2. Confirmation tests.

Cutting Tool	Coated Carbide
Cutting condition	Dry cutting
Workpiece	S45C
Cutting speed (m/min)	100, 150, 200
Feed rate (mm/rev)	0.15, 0.2, 0.25
Depth of cut (mm)	0.4, 0.6, 0.8
Nose radius (mm)	0.4, 0.8
Rake angle (degree)	−6, +11

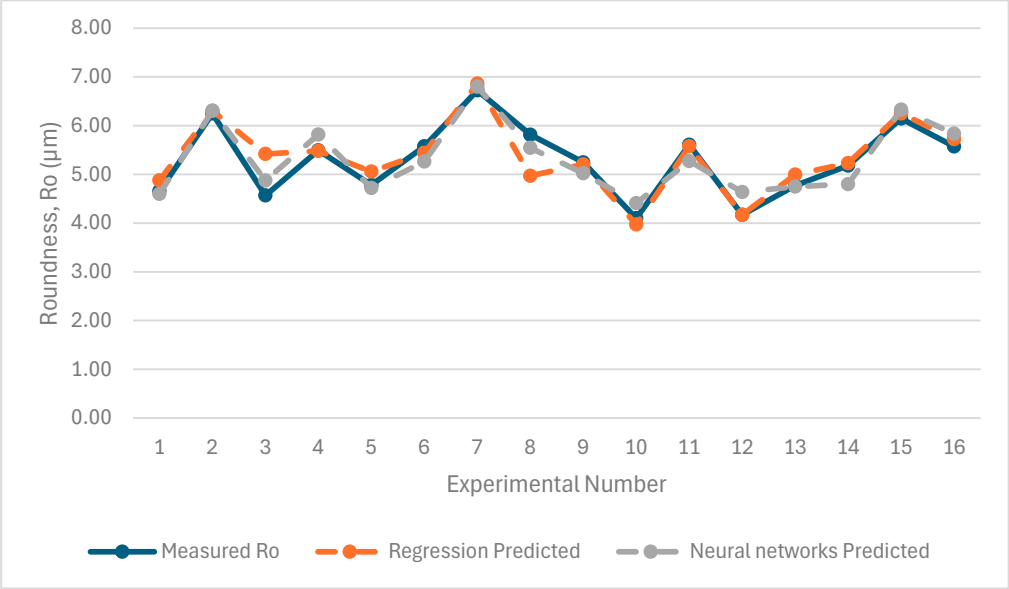


Figure 16. Illustration of measured roundness versus predicted roundness obtained from nonlinear regression model and trained neural network.

Table 3. Summarised prediction accuracy of nonlinear regression models and neural network system.

In-Process Prediction System	Prediction Accuracy			
	Average Surface Roughness (Ra)	Surface Roughness (Rz)	Straightness (St)	Roundness (Ro)
Nonlinear regression models	92.10%	92.82%	91.55%	95.52%
Trained neural network	88.08%	88.70%	90.89%	96.02%

Although Figures 13–16 demonstrate the close alignment between measured and predicted values using both the nonlinear regression model and trained neural network, there is a visible tendency suggesting potential overfitting in the neural network predictions. It is particularly evident in the higher experimental numbers, where the neural network curves follow the fluctuations of the measured values more closely than the regression model. While this may reflect high sensitivity, it could also indicate that the network has adapted too closely to the training data, potentially reducing generalisability to unseen data. Despite the high correlation coefficients observed during the validation and testing phases ($R > 0.95$), this behaviour highlights the importance of further optimisation through techniques such as cross-validation or regularisation. Moreover, the robustness of the nonlinear regression models is confirmed by their more consistent alignment with the measured values across all experimental runs, supporting their higher reliability and predictive accuracy, as reported in Table 3.

The nonlinear model outperformed in Ra, Rz, and St due to its stability and lower variance across all experimental ranges, whereas the neural network showed higher R only for Ro, suggesting possible sensitivity to noise in radial forces.

It is noticed that the nonlinear regression models have higher prediction accuracy than the trained neural network based on the experimental data in Tables 2 and 3. The highest advantage of the in-process prediction system is that all critical parameters of the average roughness, surface roughness, straightness, and roundness can be monitored, and the quality of the workpiece can be controlled during the in-process CNC turning, which can assist in reducing the production cycle time by approximately 50%, as shown in

Figure 17, since the quality control is monitored simultaneously during in-process CNC turning, which compares the CNC turning machine with the intelligent one [16,37,46,56].

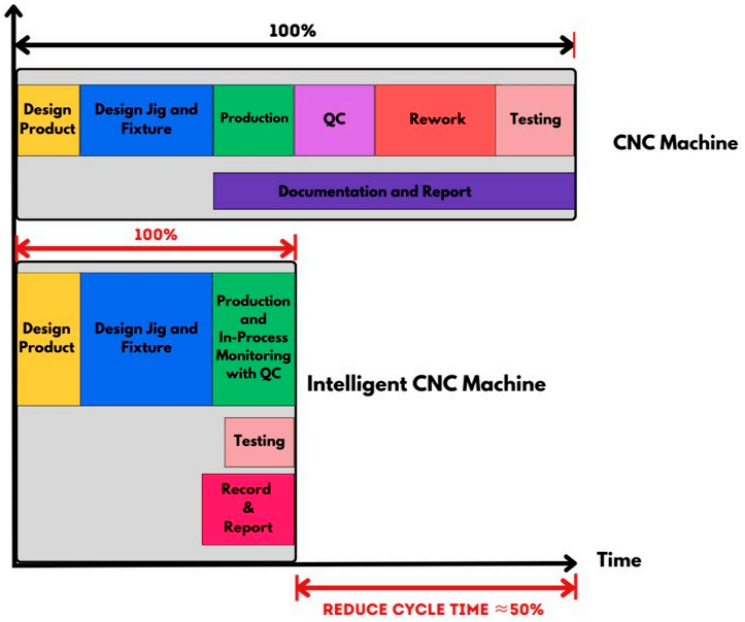


Figure 17. Comparison of production cycle time between CNC turning machine and intelligent CNC turning machine.

Figure 17 illustrates the production cycle time obtained from the CNC machine and the intelligent CNC machine. Quality control can be checked during production during in-process CNC turning by using an intelligent CNC machine, which can also record and generate the production report concurrently [4,30,39]. In-process monitoring and quality control have never been proposed before to achieve a sustainable and intelligent manufacturing system, which can be developed and implemented well by utilising the ratios of $\frac{AF_y}{AF_z}$, $\left(\frac{F_{y(dmax)}-F_{y(dmin)}}{F_{y(s)}}\right)$, and $\frac{AVF_x}{AVF_y}$. It can be concluded that all dimensions can be well identified and controlled at the same time during in-process turning with higher accuracy by applying the nonlinear regression models.

Hence, it is understood that the intelligent CNC turning machine can eliminate rejects, reworks, times and costs from a reproduction of the new parts, which can reduce greenhouse gas and energy, leading to a sustainable and intelligent manufacturing system in the near future [57–60], as shown in Figure 1. It is implied that digital transformation (DX) in terms of intelligent CNC machines is necessary to help improve green transformation (GX) and reduce time and energy consumption for sustainable and intelligent manufacturing systems, as shown in Figure 17.

6. Conclusions

To realise a sustainable and intelligent manufacturing system, the proposed intelligent machine can monitor and control the quality of the workpiece in terms of the average roughness, the surface roughness, the straightness, and the roundness simultaneously during in-process CNC turning by utilising the ratio of decomposed feed force to decomposed main force (AFy/AFz), the ratio of the peak-to-valley amplitude of decomposed feed force to its static feed force (Fy(dmax) – Fy(dmin))/Fy(s), and the ratio of the average variance of decomposed radial force to that of the decomposed feed force (AVFx/AVFy), which are obtained by adopting Daubechies wavelet transform. The nonlinear regression analyses and artificial neural network as the feed-forward neural network with back propagation

algorithm are applied to predict the in-process average roughness, surface roughness, straightness, and roundness simultaneously.

Statistical analyses have validated the experimentally obtained data before modelling the in-process prediction and training the neural network system, which are the normal test, the independent test, and the variance test, respectively. The effects of cutting conditions on those parameters, which correspond with the in-process prediction models, are explained. The experimentally obtained results showed that the average roughness, surface roughness, straightness, and roundness could be predicted well and with higher accuracy by nonlinear regression analyses compared to trained neural networks. The largest benefit of the in-process prediction system is that all critical parameters of the average roughness, surface roughness, straightness, and roundness can be monitored, and the quality of the workpiece can be controlled during the in-process CNC turning, which can aid in reducing the production cycle time and control the quality of workpiece simultaneously during in-process CNC turning.

The comparison between the CNC turning machine and an intelligent CNC turning machine has been described as beneficial, as it can monitor and control the quality of the workpiece and record and generate the production report concurrently during in-process CNC turning. It is concluded that the proposed and developed intelligent CNC turning machine can leverage intelligent machines and lead to a sustainable and intelligent manufacturing system in the near future.

Author Contributions: Conceptualization, S.T. and N.S.; methodology, S.T. and N.S.; software, S.T. and N.S.; validation, S.T. and N.S.; formal analysis, S.T. and N.S.; investigation, S.T. and N.S.; resources, S.T. and N.S.; data curation, S.T. and N.S.; writing—original draft preparation, S.T. and N.S.; writing—review and editing, A.F.; visualization, S.T. and N.S.; supervision, A.F.; project administration, A.F. All authors have read and agreed to the published version of the manuscript.

Funding: Funding from the Thailand Research Fund (TRF) and the Asahi Glass Foundation in Japan from 2019 to 2020.

Data Availability Statement: The datasets generated and analysed during the current study are available from the corresponding author upon reasonable request.

Acknowledgments: This work was financially supported by partial funding from the Thailand Research Fund (TRF) and the Asahi Glass Foundation in Japan from 2019 to 2020.

Conflicts of Interest: The authors declare no conflicts of interest.

References

1. Kumar, K.A.; Ratnam, C.; Rao, K.V.; Murthy, B.S.N. Experimental studies of machining parameters on surface roughness, flank wear, cutting forces and work piece vibration in boring of AISI 4340 steels: Modelling and optimization approach. *SN Appl. Sci.* **2019**, *1*, 26. [CrossRef]
2. Ali, S.H.R.; Mohamed, H.H.; Bedewy, M.K. Identifying Cylinder Liner Wear using Precise Coordinate Measurements. *Int. J. Precis. Eng. Manuf.* **2009**, *10*, 19–25. [CrossRef]
3. Ansari, H.R.; Zarei, M.J.; Sabbaghi, S.; Keshavarz, P. A new comprehensive model for relative viscosity of various nanofluids using feed-forward back-propagation MLP neural networks. *Int. Commun. Heat Mass Transf.* **2018**, *91*, 158–164. [CrossRef]
4. Apostolou, G.; Ntemi, M.; Paraschos, S.; Gialampoukidis, I.; Rizzi, A.; Vrochidis, S.; Kompatsiaris, I. Novel framework for quality control in vibration monitoring of CNC machining. *Sensors* **2024**, *24*, 307. [CrossRef] [PubMed]
5. Bin, H.; Kai, J.B. Digital twin-based sustainable intelligent manufacturing: A review. *Int. J. Adv. Manuf. Technol.* **2021**, *9*, 1–21. [CrossRef]
6. Liu, S.; Bao, J.; Zheng, P. A review of digital twin-driven machining: From digitisation to intellectualisation. *J. Manuf. Syst.* **2023**, *67*, 361–378. [CrossRef]
7. Aralikatti, S.S.; Ravikumar, K.N.; Kumar, H.; Nayaka, H.S.; Sugumaran, V. Comparative study on tool fault diagnosis methods using vibration signals and cutting force signals by machine learning technique. *Struct. Durab. Health Monit.* **2020**, *14*, 127. [CrossRef]

8. Ascher, S.; Sloan, W.; Watson, I.; You, S. A comprehensive artificial neural network model for gasification process prediction. *Appl. Energy* **2022**, *320*, 119289. [CrossRef]
9. Badru, D.; Singh, D.K. Analysis and effect of input parameters on surface roughness and tool flank wear in turning operation. *Int. J. Eng. Sci. Technol.* **2012**, *4*, 2759–2765.
10. Benardos, P.G.; Vosniakos, G.C. Predicting surface roughness in machining: A review. *Int. J. Mach. Tools Manuf.* **2023**, *43*, 833–844. [CrossRef]
11. Bhushan, R.K. Impact of nose radius and machining parameters on surface roughness, tool wear and tool life during turning of AA7075/SiC composites for green manufacturing. *Mech. Adv. Mater. Mod. Process.* **2020**, *6*, 1. [CrossRef]
12. Bilski, J.; Smoląg, J.; Kowalczyk, B.; Grzanek, K.; Izonin, I. Fast computational approach to the Levenberg-Marquardt algorithm for training feedforward neural networks. *J. Artif. Intell. Soft Comput. Res.* **2023**, *13*, 45–61. [CrossRef]
13. Chigirinsky, Y.L.; Krainev, D.V.; Frolov, E.M. Transformation of narratives of the cutting operation theory in passing to the «digit». *Sci. Intensive Technol. Mech. Eng.* **2024**, *6*, 3–12. [CrossRef]
14. Coit, D.W.; Jackson, B.T.; Smith, A.E. Static neural network process models: Considerations and case studies. *Int. J. Prod. Res.* **1998**, *36*, 2953–2967. [CrossRef]
15. Du, C.; Ho, C.L.; Kaminski, J. Prediction of product roughness, profile, and roundness using machine learning techniques for a hard turning process. *Adv. Manuf.* **2021**, *9*, 206–215. [CrossRef]
16. Gao, D.; Liao, Z.; Lv, Z.; Lu, Y. Multi-scale statistical signal processing of cutting force in cutting tool condition monitoring. *Int. J. Adv. Manuf. Technol.* **2015**, *80*, 1843–1853. [CrossRef]
17. Garcia Plaza, E.; Nunez Lopez, P.J.; Beamud Gonzalez, E.M. Multi-sensor data fusion for real-time surface quality control in automated machining systems. *Sensors* **2018**, *18*, 4381. [CrossRef]
18. Guo, J.; Han, R. A united model of diametral error in slender bar turning with a follower rest. *Int. J. Mach. Tools Manuf.* **2006**, *46*, 1002–1012. [CrossRef]
19. Han, R.; Cui, B.; Guo, J. In-Process Monitoring of Dimensional Errors in Turning Slender Bar Using Artificial Neural Networks. *Comput. Support. Coop. Work. Des.* **2006**, *4402*, 277–286. [CrossRef]
20. Hu, Z.; Jiang, G.; Mei, X.; Yun, X.; Zhang, Y. Online prediction of milling inner hole roundness error based on accurate SSEM value extraction. *Shock. Vib.* **2019**, *2019*, 6049316. [CrossRef]
21. Hua, Y.; Liu, Z. Effects of cutting parameters and tool nose radius on surface roughness and work hardening during dry turning Inconel 718. *Int. J. Adv. Manuf. Technol.* **2018**, *96*, 2421–2430. [CrossRef]
22. Ivanova, T.N.; Muyzemnek, A.Y. Determining the modes of layerwise laser welding of corrosion-resistant steel plates. University proceedings. *Volga Region. Eng. Sci.* **2023**, *1*, 159–170. (In Russian) [CrossRef]
23. Jáuregui, J.C.; Reséndiz, J.R.; Thenozhi, S.; Szalay, T.; Jacsó, Á.; Takács, M. Frequency and time-frequency analysis of cutting force and vibration signals for tool condition monitoring. *IEEE Access* **2018**, *6*, 6400–6410. [CrossRef]
24. Kanovic, Z.; Vukelic, D.; Simunovic, K.; Prica, M.; Saric, T.; Tadic, B.; Simunovic, G. The modelling of surface roughness after the ball burnishing process with a high-stiffness tool by using regression analysis, artificial neural networks, and support vector regression. *Metals* **2022**, *12*, 320. [CrossRef]
25. Kasim, M.S.; Hafiz, M.S.A.; Ghani, J.A.; Haron, C.H.C.; Izamshah, R.; Sundi, S.A.; Mohamed, S.B.; Othman, I.S. Investigation of surface topology in ball nose end milling process of Inconel 718. *Wear* **2019**, *426*, 1318–1326. [CrossRef]
26. Khandey, U. Optimization of Surface Roughness, Material Removal Rate and Cutting Tool Flank Wear in Turning Using Extended Taguchi Approach. Ph.D. Thesis, National Institute of Technology, Rourkela, India, 28 May 2009.
27. Kilic, B.; Aguirre, A.; Raman, S. Inspection of the cylindrical surface feature after turning using coordinate metrology. *Int. J. Mach. Tools Manuf.* **2007**, *47*, 1893–1903. [CrossRef]
28. Kusiak, A. Smart manufacturing must embrace big data. *Nature* **2018**, *554*, 23–25. [CrossRef]
29. Kwak, J.S. Application of wavelet transform technique to detect tool failure in turning operations. *Int. J. Adv. Manuf. Technol.* **2006**, *28*, 1078–1083. [CrossRef]
30. Liang, S.Y.; Hecker, R.L.; Landers, R.G. Machining process monitoring and control: The state-of-the-art. *J. Manuf. Sci. Eng.* **2004**, *126*, 297–310. [CrossRef]
31. Liotto, G.; Wang, C. Straightness measurement of a long guide way A comparison of dual-beam laser technique and optical collimator. In Proceedings of the 2nd International Symposium on Precision Mechanical Measurements, Beijing, China, 24–28 August 2004.
32. Lu, C. Study on prediction of surface quality in machining process. *J. Mater. Process. Technol.* **2008**, *205*, 439–450. [CrossRef]
33. Lu, Y. Industry 4.0: A survey on technologies, applications and open research issues. *J. Ind. Inf. Integr.* **2017**, *6*, 1–10. [CrossRef]
34. Manjunath, K.; Tewary, S.; Khatri, N.; Cheng, K. Monitoring and predicting the surface generation and surface roughness in ultraprecision machining: A critical review. *Machines* **2021**, *9*, 369. [CrossRef]
35. Mayer, R.; Phan, A.; Cloutier, G. Prediction of diameter errors in bar turning: A computationally effective model. *Appl. Math. Model.* **2000**, *24*, 943–956. [CrossRef]

36. Moreira, L.C.; Li, W.D.; Lu, X.; Fitzpatrick, M.E. Supervision controller for real-time surface quality assurance in CNC machining using artificial intelligence. *Comput. Ind. Eng.* **2019**, *127*, 158–168. [CrossRef]
37. Nallusamy, S. Enhancement of productivity and efficiency of CNC machines in a small scale industry using total productive maintenance. *Int. J. Eng. Res. Afr.* **2016**, *25*, 119–126. [CrossRef]
38. Ntemi, M.; Paraschos, S.; Karakostas, A.; Gialampoukidis, I.; Vrochidis, S.; Kompatsiaris, I. Infrastructure monitoring and quality diagnosis in CNC machining: A review. *CIRP J. Manuf. Sci. Technol.* **2022**, *38*, 631–649. [CrossRef]
39. Parenti, P.; Leonesio, M.; Bianchi, G. Model-based adaptive process control for surface finish improvement in traverse grinding. *Mechatronics* **2016**, *36*, 97–111. [CrossRef]
40. Płodzień, M.; Żyłka, Ł.; Stoić, A. Modelling of the face-milling process by toroidal cutter. *Materials* **2023**, *16*, 2829. [CrossRef]
41. Rahman, M.A.; Saleh, T.; Jahan, M.P.; McGarry, C.; Chaudhari, A.; Huang, R.; Tauhiduzzaman, M.; Ahmed, A.; Mahmud, A.A.; Bhuiyan, M.S.; et al. Review of intelligence for additive and subtractive manufacturing: Current status and future prospects. *Micromachines* **2023**, *14*, 508. [CrossRef]
42. Raut, M.; Verma, D.D.S. To improve quality and reduce rejection level through quality control. Int. J. Recent Innov. *Trends Comput. Commun.* **2017**, *5*, 764–768.
43. Selvaraj, P.; Radhakrishnan, P.; Adithan, M. An integrated approach to design for manufacturing and assembly based on reduction of product development time and cost. *Int. J. Adv. Manuf. Technol.* **2009**, *42*, 13–29. [CrossRef]
44. Shawky, A.M.; Elbestawi, M.A. In-process evaluation of workpiece geometrical tolerances in bar turning. *Int. J. Mach. Tools Manuf.* **1996**, *36*, 33–46. [CrossRef]
45. Srinivasan, R.S.; Wood, K.L.; McAdams, D. Functional tolerancing: A design for manufacturing methodology. In Proceedings of the In International Design Engineering Technical Conferences and Computers and Information in Engineering Conference, Boston MA, USA, 17–20 September 1995; Volume 17179, pp. 465–482.
46. Stathatos, E.; Tzimas, E.; Benardos, P.; Vosniakos, G.C. Convolutional neural networks for raw signal classification in CNC turning process monitoring. *Sensors* **2024**, *24*, 1390. [CrossRef] [PubMed]
47. Subramanian, K. Finishing methods using multipoint or random cutting edges. In *Surface Engineering*; ASM International: Almere, The Netherland, 1994; pp. 90–109.
48. Sukthomya, W.; Tannock, J.D. Taguchi experimental design for manufacturing process optimisation using historical data and a neural network process model. *Int. J. Qual. Reliab. Manag.* **2005**, *22*, 485–502. [CrossRef]
49. Sung, A.N.; Ratnam, M.M.; Loh, W.P. Effect of tool nose profile tolerance on surface roughness in finish turning. *Int. J. Adv. Manuf. Technol.* **2015**, *76*, 2083–2098. [CrossRef]
50. Tangjitsitcharoen, S. Intelligent Monitoring of Tool Wear and Quality Control of Roughness with Roundness in CNC Turning. *Int. J. Adv. Manuf. Technol.* **2024**, *135*, 2337–2354. [CrossRef]
51. Tangjitsitcharoen, S.; Chanthana, D. In-process prediction of roundness based on dynamic cutting forces. *Int. J. Adv. Manuf. Technol.* **2017**, *94*, 2229–2238. [CrossRef]
52. Tangjitsitcharoen, S.; Haruetai, L. Intelligent monitoring and prediction of tool wear in CNC turning by utilising wavelet transform. *Int. J. Adv. Manuf. Technol.* **2018**, *99*, 2219–2230. [CrossRef]
53. Tangjitsitcharoen, S.; Laiwatthanapaisan, W. Straightness Prediction in CNC Turning Process for Carbon Steel and Aluminum Workpieces Applying Artificial Neural Networks. *Int. J. Mach. Learn. Comput.* **2022**, *12*, 1098. [CrossRef]
54. Tangjitsitcharoen, S.; Samanmit, K. Monitoring of chip breaking and surface roughness in computer numerical control turning by utilising wavelet transform of dynamic cutting forces. *J. Eng. Manuf.* **2017**, *231*, 2479–2494. [CrossRef]
55. Wang, S.; Wan, J.; Zhang, D.; Li, D.; Zhang, C. Towards smart factory for industry 4.0: A self-organised multi-agent system with big data based feedback and coordination. *Comput. Netw.* **2016**, *101*, 158–168. [CrossRef]
56. Wong, S.Y.; Chuah, J.H.; Yap, H.J. Technical data-driven tool condition monitoring challenges for CNC milling: A review. *Int. J. Adv. Manuf. Technol.* **2020**, *107*, 4837–4857. [CrossRef]
57. Wang, X.; Da, Z.J.; Balaji, A.K.; Jawahir, I.S. Performance-based predictive models and optimization methods for turning operations and applications: Part 3—Optimum cutting conditions and selection of cutting tools. *J. Manuf. Process.* **2007**, *9*, 61–74. [CrossRef]
58. Yang, B.D.; Menq, C.H. Compensation for form error of end-milled sculptured surfaces using discrete measurement data. *Int. J. Mach. Tools Manuf.* **1993**, *33*, 725–740. [CrossRef]
59. Yoon, M.C.; Chin, D.H. Cutting force monitoring in the endmilling operation for chatter detection. *Proc. Inst. Mech. Eng. Part B J. Eng. Manuf.* **2005**, *219*, 455–465. [CrossRef]
60. Zębala, W.; Plaza, M. Comparative study of 3-and 5-axis CNC centers for free-form machining of difficult-to-cut material. *Int. J. Prod. Econ.* **2014**, *158*, 345–358. [CrossRef]

Disclaimer/Publisher's Note: The statements, opinions and data contained in all publications are solely those of the individual author(s) and contributor(s) and not of MDPI and/or the editor(s). MDPI and/or the editor(s) disclaim responsibility for any injury to people or property resulting from any ideas, methods, instructions or products referred to in the content.